Difference Differential Equations for a Resonator with a Very Thin Nonlinear Medium

L. A. Lugiato and F. Prati

CNISM and Dipartimento di Fisica e Matematica, Università dell'Insubria, Via Valleggio 11, 22100 Como, Italy

(Received 21 December 2009; published 9 June 2010)

We derive from the classic Maxwell-Bloch equations a set of difference-differential equations valid, in general, when the length of the nonlinear medium in the optical cavity is much smaller than a wavelength. Such equations provide an elegant and simple framework in which the case of Fabry-Perot and ring cavity can be discussed in a unified way. We outline a complete scenario for the multimode laser instability in the Fabry-Perot case, illustrating the results for parameter values appropriate to quantum cascade lasers. Our approach can have a relevant impact also on the study of dynamical instabilities in external cavity semiconductor lasers, including multiple quantum well or quantum-dot structures.

DOI: 10.1103/PhysRevLett.104.233902 PACS numbers: 42.65.Sf, 42.55.Px, 42.60.Da

The last 30 years witnessed a flourishing development of theoretical and experimental activities in the area of temporal and spatial instabilities in general and in nonlinear optical systems in particular (see, e.g., [1–3]). Complete models which include time + 3D in space are extremely difficult to handle numerically even when the nonlinear medium is enclosed in an optical cavity. A tractable configuration, which has been extensively studied, is that of ring cavity models in the single-longitudinal mode approximation, because one can neglect the longitudinal variable z and therefore reduce to time + 2D.

The case of Fabry-Perot (FP) cavity is, however, substantially more complex than that of ring cavity, because one must take into account the left- and the right-propagating fields and the standing wave effects which arise from their superposition. Literature on FP instabilities is substantially less extended (see, e.g., [4,5]).

Here we show that a dramatic simplification can be introduced when the medium has a longitudinal extension w much smaller than the carrier wavelength λ, which is the situation in engineered devices such as quantum well devices. Starting from the classic context of the Maxwell-Bloch Equations (MBEs), we show that since the propagation in the empty part of the cavity is trivial, the MBEs can be lumped in general into an elegant set of difference-differential equations (DDEs) in which the longitudinal variable z does not appear any more.

The DDEs introduced for the ring cavity in the pioneering works of Ikeda [6(a),6(b)] played a crucial role in the prediction and in the analysis of optical chaos. Much more recently, a model similar to Ikeda's was derived and applied to the study of passive mode locking in semiconductor lasers [7]. Yet, those models are valid only in the rate equation approximation [6(a),7] or in the dispersive Kerr limit [6(b)]. A generalization of the latter case to the FP configuration was provided in [6(c)].

By contrast, in the derivation of our DDEs for the case $w \ll \lambda$ we do not make any assumption on the relaxation rates of the variables. Yet, our equations are much simpler than those of [6] for the MBEs. This feature of elegance and simplicity brings also another important bonus: the equations for the FP case are only slightly more complex than for the ring cavity, because the forward and backward fields can be lumped into a single field and standing wave effects do not enter into play.

By using this set of DDEs, the computer time is drastically reduced. Even in the context of the plane wave approximation, i.e., neglecting the transverse variables x and y, the reduction is on the order of a factor 100.

We derive the DDEs for both the FP and the ring cavity, but we devote more attention to the FP case which in this case can be treated in a simple way for the first time. For the sake of brevity, we limit ourselves to the case that the medium is in resonance with the cavity and, when there is an input field injected into the cavity, it is also resonant. The generalization to the nonresonant case does not present difficulties.

We consider a FP cavity of length $L \gg \lambda$ containing a nonlinear medium of thickness $w \ll \lambda$ centered at $z = \bar{z}$. The system is described by a set of MBEs that follow from those of [4,8] assuming (as implied by the condition $w \ll \lambda$) that the atomic variables P (polarization) and D (population difference) depend only on the value of the forward and backward fields $E_{F,B}$ at $z = \bar{z}$ and that the source term in the Maxwell equation is δ like in z

$$e^{ik_0 z}\left[\frac{\partial E_F}{\partial z} + \frac{1}{v}\frac{\partial E_F}{\partial t}\right] + e^{-ik_0 z}\left[-\frac{\partial E_B}{\partial z} + \frac{1}{v}\frac{\partial E_B}{\partial t}\right] = \alpha\sigma w P(t)\delta(z-\bar{z}), \tag{1}$$

$$\frac{dP}{dt} = \gamma^{-1}[F(t)D(t) - P(t)], \tag{2}$$

$$\frac{dD}{dt} = -\gamma\left[\frac{F(t)P^*(t) + F^*(t)P(t)}{2} + D(t) - 1\right], \tag{3}$$

with

$$F(t) = e^{i\phi}E_F(\bar{z}, t) + e^{-i\phi}E_B(\bar{z}, t), \tag{4}$$

and $\phi = k_0\bar{z}$ (mod π). In the above equations α is the unsaturated gain/absorption coefficient per unit length, $\sigma = 1$ for an amplifier medium and $\sigma = -1$ for an absorber, and $k_0 = 2\pi/\lambda$. Time is scaled to the inverse of $\sqrt{\gamma_\parallel \gamma_\perp}$ where $\gamma_\perp$ and $\gamma_\parallel$ are the decay rates of P and D, respectively. Hence, $v = c/\sqrt{\gamma_\parallel \gamma_\perp}$ and $\gamma = \sqrt{\gamma_\parallel/\gamma_\perp}$. Perfect resonance between the carrier frequency and the atoms has been assumed and all the quantities E_F, E_B, P D have been properly normalized.

If we introduce the variables $t' = t - z/v$ and $z' = z$, and write $E_F(z, t) = \tilde{E}_F(z', t') = E_F(z', t' + z'/v)$, $E_B(z, t) = \tilde{E}_B(z', t') = E_B(z', t' + z'/v)$, Eq. (1) becomes

$$\frac{\partial \tilde{E}_F}{\partial z'} + e^{-2ik_0 z'}\left[-\frac{\partial \tilde{E}_B}{\partial z'} + \frac{2}{v}\frac{\partial \tilde{E}_B}{\partial t'}\right] = \alpha\sigma w e^{-ik_0 z'} P(t' + z'/v)\delta(z' - \bar{z}). \quad (5)$$

Now we integrate this equation in z' first from $z' = 0$ to $z' = \bar{z}$ and then from $z' = \bar{z}$ to $z' = L$. In both cases the contribution of the terms with $\tilde{E}_B$ vanishes, provided $\bar{z}$, $L - \bar{z} \gg \lambda$, because the variation of those terms is much slower than the variation of the exponential term $e^{-2ik_0 z'}$. In terms of the field E_F we have

$$E_F(L, t' + L/v) - E_F(\bar{z}, t' + \bar{z}/v) = E_F(\bar{z}, t' + \bar{z}/v) - E_F(0, t') = \Gamma P(t' + \bar{z}/v), \quad (6)$$

with $\Gamma = (\alpha\sigma w/2)e^{-i\phi}$. By proceeding in a similar way with the variables $t'' = t + z/v$ and $z'' = z$, we have

$$E_B(\bar{z}, t'' - \bar{z}/v) - E_B(L, t'' - L/v) = E_B(0, t'') - E_B(\bar{z}, t'' - \bar{z}/v) = \Gamma^* P(t'' - \bar{z}/v). \quad (7)$$

The boundary conditions of the FP resonator with two plane mirrors of reflectivity $R = 1 - T$ are [9]

$$E_F(0, t) = \sqrt{R} E_B(0, t) + Ty, \qquad E_B(L, t) = \sqrt{R} E_F(L, t), \quad (8)$$

where y is the normalized amplitude of a perfectly resonant external field which possibly enters the cavity through the mirror at $z = 0$. By setting $t' + \bar{z}/v \to t$ in Eq. (6) and $t'' - \bar{z}/v \to t$ in Eq. (7) and expressing E_F and E_B at $z = 0$ and $z = L$ in terms of E_F and E_B at $z = \bar{z}$, we can transform the boundary conditions (8) in two coupled maps for $E_F(\bar{z}, t)$ and $E_B(\bar{z}, t)$. Once inserted one into the other, they yield two separate maps for E_F and E_B, from which we can obtain a single map for the field F defined by Eq. (4). In the limit $T \ll 1$, $\alpha w = O(T)$ and keeping only terms up to first order in T, it reads

$$F(t) = RF(t - \tau) + T\{\mu y + C\sigma[P(t) + P(t - \tau)] + \nu C\sigma[e^{2i\phi}P(t - \bar{\tau}) + e^{-2i\phi}P(t - \tau + \bar{\tau})]\}, \quad (9)$$

where $C = \alpha w/T$, $\mu = 2\cos\phi$, $\nu = 1$, and $\tau = 2L/v$ is the cavity round-trip time, while $\bar{\tau} = 2\bar{z}/v$ is the time taken by light to travel from the nonlinear medium to the mirror in $z = 0$ and back.

A similar map can be obtained considering a ring cavity of length $\mathcal{L}$ with two partially reflecting mirrors. In that case obviously the parameters ϕ and $\bar{\tau}$ disappear because, if the electric field is a traveling wave, the position $\bar{z}$ of the nonlinear medium is irrelevant. By starting from Eqs. (1)–(4) with E_F only and 2α instead of α, one arrives at Eq. (9) with $\mu = 1$, $\nu = 0$, and $\tau = \mathcal{L}/v$. A similar equation for a ring cavity was derived in [10] under the assumption of nonlinear medium much shorter than the cavity length. Indeed in a ring cavity it is not necessary to assume that the medium is much shorter than the wavelength because of the traveling wave nature of the electric field.

With the appropriate choice of the parameters μ and ν, the set of DDEs (2), (3), and (9) describes both a FP resonator and a ring cavity in the limit of thin nonlinear medium. In the following we will focus on the case of a laser ($\sigma = 1$) without an injected field ($y = 0$). A quantum cascade laser (QCL) with coated surfaces would be particularly suited to be modeled with our equations, because the high reflectivity would allow one to build an active region with few gain periods. Since the thickness of a single period is about 50 nm and the emission wavelength is about 10 μm, our assumption of active region thin with respect to the period of the standing wave would be well satisfied by such a laser. For this reason in this Letter we assume high mirror reflectivity ($T = 0.01$) and $\gamma = 0.365$, a value suitable for a quantum cascade laser [11].

In the stationary solution of the DDEs only the resonant mode is active and one has

$$|x|^2 = 2C(1 + \nu\cos 2\phi) - 1, \quad (10)$$

where x is the stationary value of F. The laser threshold is $2C_{\mathrm{th},0} = 1$ for a ring cavity and $4C_{\mathrm{th},0} = 1/\cos^2\phi$ for a FP resonator, i.e., in that case it depends on the position of the active region. The threshold is minimum when the active region is positioned at an antinode of the standing wave profile ($\cos^2\phi = 1$). This is in contrast with the case of a medium of length $w \gg \lambda$, in which the steady-state solution does not depend on the position of the sample in the cavity [8].

We perform a standard linear stability analysis of the stationary solution by introducing the fluctuations $\delta X(t) = \delta X_0 e^{\lambda t}$ with $X = F, F^*, P, P^*, D$. In the limit $T \ll 1$ we can solve the problem perturbatively by setting $\lambda = \lambda_n = \lambda_n^{(0)} + T\lambda_n^{(1)} + O(T^2)$, where $\lambda_n^{(0)} = -i\omega_n$ and $\omega_n = 2\pi n/\tau$, ($n = 0, \pm 1, \ldots$) is the angular frequency of the empty cavity longitudinal mode of index n (the resonant mode corresponds to $n = 0$). Since $\lambda_n^{(0)}$ is purely imaginary, the stability of the stationary solution is determined by the sign of the real part of the first order corrections $\lambda_n^{(1)}$, which can be obtained from the linearized equations at first order in T

$$[\mathcal{A}\beta_n^+ - \mathcal{C}(1 + \lambda_n^{(1)}\tau)]\delta F_0 + \mathcal{B}\beta_n^+ x^2 \delta F_0^* = 0, \quad (11)$$

$$\mathcal{B}\,\beta_n^- x^{*2}\delta F_0 + [\mathcal{A}\beta_n^- - \mathcal{C}(1 + \lambda_n^{(1)}\tau)]\delta F_0^* = 0, \quad (12)$$

with $\mathcal{A} = 2(1 - i\gamma\omega_n)(\gamma - i\omega_n) + i\gamma^2|x|^2\omega_n$, $\mathcal{B} = \gamma(i\gamma\omega_n - 2)$, and $\mathcal{C} = 2(1 - i\gamma\omega_n)[(1 - i\gamma\omega_n)\times(\gamma - i\omega_n) + \gamma|x|^2]$. The coefficients $\beta_n^\pm$ represent the ratio of the intensities of the modes $\pm n$ to that of the resonant mode at $z = \bar{z}$.

In a ring cavity $\beta_n^\pm = 1$ because the modes are traveling waves. This implies that we can write two independent equations for the real and imaginary parts of δF_0 and distinguish [2] between a phase eigenvalue, which does not give rise to any instability, and an amplitude eigenvalue, which coincides with that of the classic Risken-Nummedal-Graham-Haken (RNGH) instability [12]. An example of instability domain is shown in Fig. 1.

In a FP cavity the coefficients $\beta_n^\pm$ are given by

$$\beta_n^\pm = \cos^2(\phi \pm \pi n r)/\cos^2\phi, \quad (13)$$

where the parameter $r = \bar{\tau}/\tau = \bar{z}/L$ is the relative position of the nonlinear medium inside the cavity. If the nonlinear medium is positioned exactly at one antinode of the standing wave ($\phi = 0$), we have $\beta_n^\pm = \cos^2(\pi n r) \equiv \beta_n$. Amplitude and phase instabilities are still decoupled because $\beta_n^+ = \beta_n^-$ but, unlike in the ring cavity, the shape of the instability domains depends on the modal index n through the coefficients β_n, which range from 0 to 1. For $\beta_n = 1$ the instability domain coincides with that of the ring cavity, for smaller β_n it moves to the right and the instability threshold rapidly increases. This means that a variety of new RNGH-like instability scenarios are possible in the FP cavity, depending on r. Here we focus on the simplest case $r = 1/2$, i.e., active medium placed exactly at the center of the cavity. In that case β_n can take only two values: 1 for even n, and 0 for odd n. For $\beta_n = 0$ there is no instability. Thus, the RNGH instability domain of Fig. 1 is valid for both types of cavity, but in the FP cavity the solution can be destabilized only by even modes. The RNGH instability has been recently observed in a QCL laser in a FP configuration [11].

We have integrated the DDEs with $C/C_{\mathrm{th},0} = 12$ and $\tau = 3$ ($\omega_2 \simeq 4.19$) for both types of cavity and $\phi = 0$, $r = 1/2$ for the FP cavity. With that choice the stationary solution is unstable with respect to modes $n = \pm 2$. The pulses obtained with the two types of cavity are almost perfectly identical, and they also coincide with those obtained integrating the standard MBEs, where it is assumed that the nonlinear medium fills the cavity. This result stems from the choice of r and τ. For other values of those parameters the two types of cavity will differ both for the instability threshold and for the order of the modes involved in the dynamics.

For a generic FP resonator with $\phi \neq 0$ the amplitude and phase instabilities are no longer decoupled, and new instabilities may arise due to the fact that mode $n = 0$, which is resonant with the atoms, is not necessarily the mode with maximum gain. This occurs because, although

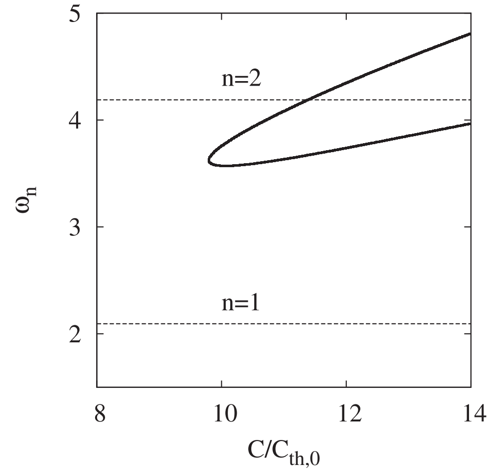

FIG. 1. Instability domain of the stationary solution of Eqs. (2), (3), and (9) for a ring cavity and a FP cavity with $\phi = 0$, $r = 1/2$. For a given C the solution is unstable against mode n if ω_n lies between the two curves. For the FP cavity n must be an even number. The dashed lines show the values of ω_1 and ω_2 for $\tau = 3$.

the resonant mode $n = 0$ has the maximum "spectral" gain, a mode with a different index could experience more "spatial" gain, because its standing wave pattern matches better the position of the active region. Therefore, in addition to the stationary solution (10), Eqs. (2), (3), and (9) admit also other stable single-mode solutions with stationary intensity, where only one nonresonant mode $n \neq 0$ is active. The threshold for such solutions is $4C_{\mathrm{th},n} = (1 + \omega_n^2\gamma^2)/\cos^2(\phi + \pi n r)$, where the numerator displays the parabolic increase of the threshold with the frequency typical of two-level atoms, but the denominator, if $\phi \neq 0$, can compensate for it and make the threshold for a mode of index $n \neq 0$ smaller than that for $n = 0$.

Let us consider for instance a FP cavity with $\phi = -\pi/5$ and $r = 0.1125$. The instability domain of the stationary solution $n = 0$ with respect to mode $n = 1$ is shown in Fig. 2(a). A new instability domain besides the RNGH-like one appears for smaller values of pump and frequency. The stationary solution $n = 0$ is unstable with respect to mode $n = 1$ already at threshold when the frequency ω_1 is not too much detuned from resonance.

Depending on the cavity length, we have two different scenarios: for shorter cavities ($\omega_1 > 3.873$) the RNGH instability, for longer cavities ($1.765 < \omega_1 < 2.2$) a novel instability, which occurs much closer to threshold, and causes a switch from mode $n = 0$ to mode $n = 1$ as C increases, as shown in Fig. 2(b).

The relevant point is that the switch is not abrupt because there is a range of values of C for which none of the modes is stable and the output is oscillatory. In that case the squares represent the minima and maxima of the oscillations. After the laser has switched to mode $n = 1$, the opposite switch is observed if C is decreased. The dashed lines represent the stationary intensities of the two single-mode solutions $n = 0$ and $n = 1$. Over a large range of

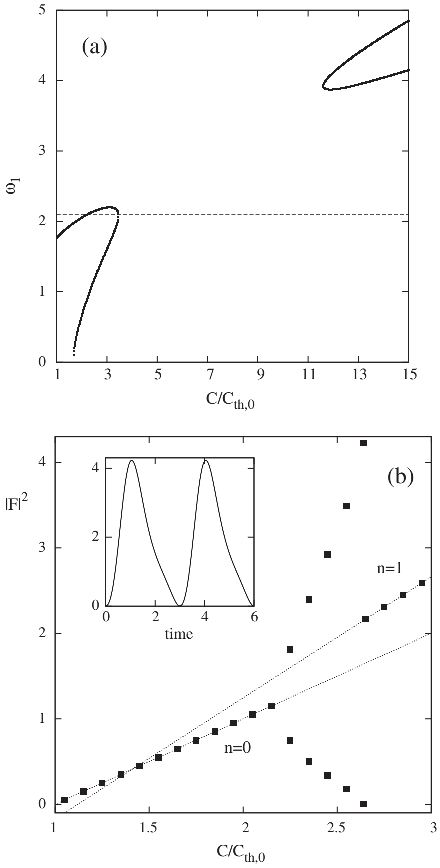

FIG. 2. (a) Instability domains of the stationary solution of Eqs. (2), (3), and (9) with respect to mode $n = 1$ in a FP cavity with $\phi = -\pi/5$ and $r = 0.1125$. (b) Output intensity for different C and $\tau = 3$, which corresponds to the dashed line of (a). The inset shows the pulsations for $C = 2.64C_{\mathrm{th},0}$.

values of C the laser emits mode $n = 0$ although the intensity of mode $n = 1$ would be larger.

In conclusion, for a nonlinear medium of length w much smaller than the wavelength λ we have cast the classic MBEs into a very advantageous difference-differential equations configuration, which allows us to treat the FP case in parallel to that of a ring cavity. This has allowed us to obtain in a straightforward way a complete picture of the instability scenario for a FP laser, including the case of the classic RNGH multimode instability (which is much richer in the FP case) and a novel low threshold self-pulsing instability which is exclusive for the FP configuration.

Our approach can have the most relevant impact in the case of three spatial dimensions, in the study of phenomena of outstanding interest for applications, e.g., the generation of pulses localized in 3D and time (light bullets). The substantial reduction in computer time represents in this case the crucial step which enables one to engineer the parameters (such as $\bar{z}$, τ, $\bar{\tau}$) to obtain the desired spatio-temporal behavior. 3D models include the transverse variables x and y via the transverse Laplacian which describes diffraction in the paraxial approximation. The most natural configuration is that of external cavity semiconductor lasers such as the VECSELs [13], which contain multiple quantum well or quantum-dot regions. For example, it can advantageously be applied to the VECSEL with saturable absorber [14]. The procedure to derive the DDEs, that we described for the MBEs, can be straightforwardly generalized to semiconductor models, both in the rate equation approximation and including the material polarization, as it will be explicitly shown elsewhere.

We thank one of the referees for informing us of Ref. [10].

[1] N. B. Abraham, P. Mandel, and L. M. Narducci, in *Progress in Optics* (North-Holland, Amsterdam, 1988), Vol. 25, p. 3ff; C. O. Weiss and R. Vilaseca, *Dynamics of Lasers* (VCH, Weinheim, 1991); Ya. I. Khanin, *Principles of Laser Dynamics* (Elsevier, New York, 1995); W. J. Firth, in *Self-organization in Optical Systems with Applications to Information Technology* (Springer-Verlag, Berlin, 1995), p. 69ff; P. Mandel, *Theoretical Problems in Cavity Nonlinear Optics* (Cambridge University Press, Cambridge, UK, 1997); F. T. Arecchi, S. Boccaletti, and P. L. Ramazza, Phys. Rep. **318**, 1 (1999).
[2] L. A. Lugiato and L. M. Narducci, in *Fundamental Systems in Quantum Optics* (Elsevier, New York, 1992) p. 941ff.
[3] L. A. Lugiato, M. Brambilla, and A. Gatti, in *Advances in Atomic, Molecular, and Optical Physics* (Academic Press, San Diego, 1999), Vol. 40, p. 229ff.
[4] H. M. Gibbs, *Optical Bistability: Controlling Light with Light* (Academic Press, Orlando, 1985), p. 47.
[5] H. J. Carmichael, Opt. Acta **27**, 147 (1980); L. W. Casperson, Phys. Rev. A **21**, 911 (1980).
[6] (a) K. Ikeda, Opt. Commun. **30**, 257 (1979); (b) K. Ikeda, H. Daido, and O. Akimoto, Phys. Rev. Lett. **45**, 709 (1980); (c) K. Ikeda and M. Mizuno, IEEE J. Quantum Electron. **21**, 1429 (1985).
[7] A. G. Vladimirov and D. Turaev, Phys. Rev. A **72**, 033808 (2005).
[8] L. A. Lugiato and L. M. Narducci, Z. Phys. B **71**, 129 (1988).
[9] S. L. Mc Call, Phys. Rev. A **9**, 1515 (1974).
[10] P. W. Milonni, M. L. Shih, and J. R. Ackerhalt, *Chaos in Laser–Matter Interactions* (World Scientific Publishing Company, Singapore, 1987), pp. 162–167.
[11] A. Gordon *et al.*, Phys. Rev. A **77**, 053804 (2008). Here the observed instability threshold was much lower than predicted by the RNGH theory, and that behavior was attributed to the presence of saturable absorption.
[12] H. Risken and K. Nummedal, J. Appl. Phys. **39**, 4662 (1968); R. Graham and H. Haken, Z. Phys. **213**, 420 (1968); E. M. Pessina, G. Bonfrate, F. Fontana, and L. A. Lugiato, Phys. Rev. A **56**, 4086 (1997); T. Voigt, M. Lenz, F. Mitschke, E. Roldán, and G. J. de Valcárcel, Appl. Phys. B **79**, 175 (2004).
[13] X. Hachair *et al.*, Opt. Express **16**, 9519 (2008).
[14] U. Keller and A. C. Tropper, Phys. Rep. **429**, 67 (2006).